Clays and Clay Minerals, Vol. 60, No. 4, 363–373, 2012.

CONFORMATIONAL EFFECTS OF ADSORBED POLYMER ON THE SWELLING BEHAVIOR OF ENGINEERED CLAY MINERALS

SUNGHO KIM[1], MICHAEL A. MOTYKA[2], ANGELICA M. PALOMINO[1,*], AND NIKOLAS J. PODRAZA[3]

[1] Department of Civil and Environmental Engineering, University of Tennessee, Knoxville, TN 37996, USA
[2] Department of Engineering Science and Mechanics, Pennsylvania State University, University Park, PA 16802, USA
[3] Department of Physics and Astronomy, University of Toledo, 2801 W. Bancroft St. Mailstop 111, Toledo, OH 43606, USA

Abstract—The conformational behavior of polymers in clay-polymer nanocomposites (CPN) is not fully understood because of the many factors involved. The purpose of the present study was to investigate the conformational behavior of a polymer at the micro- and meso-scales in order to predict the behavior of tunable CPN. The study used a pH-responsive polymer, polyacrylamide, which has time-dependent hydrolysis response properties, to examine micro-scale conformational behavior of the polymer adsorbed on representative clay-mineral surfaces, SiO_2 and Al_2O_3. A nanocomposite and a microcomposite were used to link meso-scale CPN behavior to micro-scale polymer conformation. The conformational behavior was characterized using *in situ*, real-time spectroscopic ellipsometry. The contracted coil conformation of polyacrylamide was observed at pH = 3, while extended conformation was observed at pH = 11.5 on both SiO_2 and Al_2O_3 surfaces. At pH = 11.5, the polymer conformation changed from expanded coil to extended conformation over time. The polymer conformation changed more rapidly with the Al_2O_3 surface due to mineral dissolution at pH = 3 and 11.5. Swelling tests were conducted as functions of pH and time to link the micro-scale phenomena to meso-scale CPN behavior. The results indicated that the swelling potential of CPN corresponded to the conformation of adsorbed polyacrylamide, which varied with pH and time. The swelling potential of CPN was maximized at pH = 11.5 and decreased with decreasing pH, corresponding to the observed micro-scale conformational behavior.

Key Words—Kaolinite, Montmorillonite, pH-responsive Polymer, Polyacrylamide, Spectroscopic Ellipsometry, Swelling Potential, Tunable Clay-polymer Nanocomposites.

INTRODUCTION

Clay-polymer composites are clay mineral particles associated with adsorbed polymer molecules. They can be divided into three categories – microcomposite, intercalated nanocomposite, and exfoliated nanocomposite (Giannelis *et al.*, 1999; Alexandre and Dubois, 2000; Ray and Okamoto, 2003; Ruiz-Hitzky and van Meerbeek, 2006). Microcomposites are separated phases of clay minerals and polymer molecules without interlayer interactions between the two components. In an intercalated nanocomposite, polymer molecules are inserted into the interlayer space of clay minerals, yet the layered structure is still maintained. In an exfoliated nanocomposite, the layers are completely separated by polymer molecules. Exfoliated structures of clay minerals are often used to improve polymeric materials rather than to enhance the performance of a clay mineral by using a polymer. For example, ~1 vol.% of montmorillonite exfoliated in a matrix of poly(vinyl alcohol) enhances two-fold the Young's modulus of the polymeric system (Strawhecker and Manias, 2006). Tunable CPN with intercalated structure, the performance of which is controlled by changing an environmental trigger such as pH and ionic strength, have recently been synthesized using a responsive polymer and clay minerals (Kim and Palomino, 2011). The conformation (expansion or contraction) of the responsive polymer molecules in the tunable CPN is a function of environmental conditions, which supports the modification of CPN properties. For example, a CPN synthesized using polyacrylamide (PAM) is expected to have greater interlayer and interparticle distances, *i.e.* open fabric, at pH > 11 than at pH < 10 (Kim *et al.*, 2012). Thus, the swelling of the CPN is maximized at pH > 11. Because responsive polymer conformation controls the performance of the tunable CPN, characterization of the polymer conformation adsorbed in the CPN structure is critical.

Many factors including charge density, concentration, molecular weight, degree of ionization, acid dissociation constant, pK_a, of the ionizable group, crosslinking density, and hydrophilicity of the polymer as well as properties of the medium such as pH, ionic concentration, temperature, and counterion type and valence affect the conformation of the polymer in dilute solutions (Flory, 1953; Askadskii, 1990; Castel *et al.*, 1990; Fleer, 1993; Lee *et al.*, 1999; Lee and Lin, 2001; Wu *et al.*, 2001; Gupta *et al.*, 2002). Even though the polymer is expected to take on a particular conformation in a dilute solution, the polymer may not adopt the same conformation when adsorbed onto a clay-mineral surface. The polymer conformation at the liquid–solid interface may

* E-mail address of corresponding author:
apalomin@utk.edu
DOI: 10.1346/CCMN.2012.0600403

also be influenced by the properties of a surface such as roughness, curvature, and charge density (Michaels, 1954; Fleer, 1993). For example, a partially charged polymer tends to have expanded coil conformation in dilute solution, but a rather flat conformation on a surface with the opposite charge. In addition, surface charge heterogeneity for clay mineral edge and face surfaces may lead to complex conformational behavior of polymer molecules. For example, even if the edge area of kaolinite contributes <10% of the whole surface area, it represents ~95% of total surface charge (van Olphen, 1977). Due to a very small edge area, surface charge at the montmorillonite edges represents <5% of the total surface charge (Borchardt, 1989). Therefore, the nature of the polymer, fluid medium, and surface must all be considered in order to understand the conformational behavior of the polymer on a surface in an aqueous medium.

Ellipsometry is an optical technique for characterizing adsorbed polymer molecules on a surface (Lee and Fuller, 1984; Irene, 1993; Filippova, 1998; Schwarz *et al.*, 1999; Russev *et al.*, 2000; Fan and Advincula, 2002; Fan *et al.*, 2002; Wang *et al.*, 2004; Schmidt *et al.*, 2009). Many techniques can be used to characterize adsorbed polymer layers, such as vibrational spectroscopy, magnetic resonance, and neutron scattering (Cohen Stuart *et al.*, 1986). An advantage of ellipsometry is that it may be used to monitor the characteristics of adsorbed polymer molecules on a specular surface *in situ*. In addition, the technique can accurately capture characteristics of adsorbed polymer layers at the liquid−solid interface. The achievable resolution can be <0.1 nm, but sensitivity to film thickness can be maintained up to tens of microns.

The conformational behavior of a large-molecular-weight polymer after adsorption on a clay-mineral particle has not been studied previously because current experimental technologies limit the ability to characterize the conformation of the polymer adsorbed on a mobile, suspended surface, *i.e.* clay-mineral particles dispersed in water. This problem was overcome in the present study by using a representative surface rather than an actual clay mineral surface as an alternative to characterize adsorbed polymer conformation so that the evolution of the absorbed polymer conformation could be monitored using spectroscopic ellipsometry (SE). The purpose of the present study was to investigate time-dependent conformational behavior of a pH-responsive polymer adsorbed on two representative clay-mineral surfaces, and to link the micro-scale responses to a meso-scale property, swelling, of CPN. Real-time SE (RTSE) was used to characterize *in situ* polymer conformation on amorphous SiO_2 and nanocrystalline Al_2O_3 surfaces simulating the components of a typical clay-mineral surface. The swelling potential was measured for the microcomposite and intercalated nanocomposite synthesized as functions of pH and time.

EXPERIMENTAL STUDY

Materials

The polymer used in the present study was a polyacrylamide (PAM) obtained from Cytec Industries, Inc. (West Paterson, New Jersey, USA). The PAM was chosen because it is a commonly used water-soluble polymer and is also responsive to environmental pH changes (Caskey and Primus, 1986; Furusawa *et al.*, 1992). Specifically, the conformation of a PAM molecule depends on the surrounding fluid pH. The polymer molecule has a contracted coil conformation at acidic pH and an extended conformation at basic pH (Michaels, 1954; Al-Anazi and Sharma, 2002; Besra *et al.*, 2004). The PAM is also sensitive to ionic concentration (Shubin and Linse, 1995), although this property was not evaluated in this study because the ionic concentration was kept constant. The PAM molecular weight is ~6.0×10^6 a.m.u., and the radius of gyration of the molecule in the solution state is ~50 nm (Kim, 2011). Solutions of 0.1 M HCl and 0.1 M NaOH were used to adjust the solution pH, and the polymer was hydrolyzed to different degrees as a function of time. Given the hydrolyzed structure of the polymer (Figure 1) (Barvenik, 1994; Kurenkov, 1997; Pefferkorn, 1999; Myagchenkov and Proskurina, 2004), the degree of hydrolysis, $\tau = y/(x+y)$, was determined by acid-base titration. The chemical formula of poly(acrylic acid) was defined at $\tau = 1$.

Because RTSE analysis of mobile, dispersed clay-mineral particles yields results that are difficult to interpret, a less mobile, but representative, phase was needed. For this purpose, amorphous SiO_2 and nanocrystalline Al_2O_3 were selected, to represent the fundamental Si tetrahedral and Al octahedral structural components of clay minerals, respectively. The amorphous SiO_2 layer used was simply the native oxide of a crystalline silicon (c-Si) wafer. The nanocrystalline Al_2O_3 used was deposited *via* atomic layer deposition (ALD) onto a native oxide-covered c-Si substrate. The ALD processes are known for good conformal coatings and high uniformity. The thickness of the alumina layer across the substrate was 39.7±0.3 nm as determined by *ex situ* SE measurements. These representative surfaces were used to capture the conformation of the PAM adsorbed and its evolution, using RTSE.

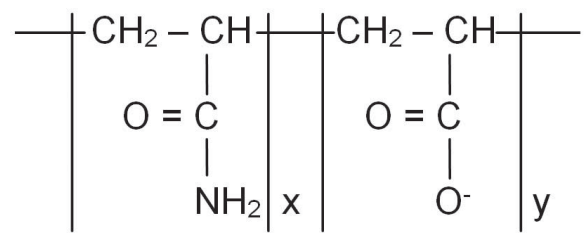

Figure 1. Structure of hydrolyzed polyacrylamide (PAM) molecule.

Real clay minerals, kaolinite and montmorillonite, were used to determine swelling potential. Kaolinite, the major component of the microcomposites studied here, exposes both silicon tetrahedral and aluminum octahedral sheets. Montmorillonite, the major component of the nanocomposites in this study, have only silicon tetrahedral sheets exposed. The kaolin used in this study was an untreated kaolin from Active Minerals International, LLC (Gordon, Georgia, USA) known commercially as Acti-Min SA-1. The kaolin was converted to a homo-ionic sodium kaolin using a conversion method modified after van Olphen (1977). A sodium bentonite from the American Colloid Company (Arlington, Illinois, USA), designated commercially as AEG powder, was used as the source of montmorillonite. The bentonite consisted mainly of montmorillonite and minor amounts of feldspar and quartz. Details of the properties of the clay minerals can be found in Kim and Palomino (2009, 2011).

The tunable CPN with intercalated structure was prepared by mixing montmorillonite with PAM at a clay-to-polymer volume ratio of 2. This volume ratio was selected to maximize the amount of intercalated structure as well as the swelling capacity (Kim and Palomino, 2011). The swelling capacity of the nanocomposite synthesized using montmorillonite and PAM is expected to be a function of the conformation of PAM. In a nanocomposite, both interlayer and interparticle spacings are modified, while microcomposite refers to the case in which only interparticle spacing modification is expected. As a comparison, a kaolinite-PAM microcomposite was synthesized by mixing kaolinite and PAM at a clay-to-polymer volume ratio of 62.5 (Kim and Palomino, 2009; Kim, 2011). The clay-to-polymer volume ratio is defined as clay volume with respect to polymer volume. The respective volume is calculated based on the mass and material density of each component.

Spectroscopic ellipsometry (SE)

Spectroscopic ellipsometry detects the change in the polarization state of light modified by a sample surface. Changes in the polarization state result in different values of the phase shift difference, Δ, and the relative amplitude ratio, ψ, which are characteristic angles of the surface reflecting the polarized light perpendicular (s-wave) and parallel (p-wave) to the plane of incidence. The fundamental relationship between Δ and ψ is given as a complex reflection coefficient ratio, ρ (Irene, 1993):

$$\rho = \tan(\psi)\exp(i\Delta) \quad (1)$$

$$\tan(\psi) = \frac{|r_p|}{|r_s|} \quad (2)$$

$$\Delta = \delta_p - \delta_s \quad (3)$$

where δ_p and δ_s are the phase angles, and r_p and r_s represent the complex amplitude reflection and Fresnel coefficients, respectively. The properties of the sample – optical properties in the form of the spectroscopic complex refractive index ($N = n + ik$) or complex dielectric function ($\varepsilon = \varepsilon_1 + i\varepsilon_2 = N^2$), and microstructural factors such as film thickness – affect the measured (Δ, ψ) spectra. Thus, the pH- and time-dependent conformational changes of adsorbed polymer molecules onto a representative mineral surface may be captured through spectroscopic measurements of these ellipsometric angles.

A multichannel ellipsometer (model RC2, J.A. Woollam Co., Inc., Lincoln, Nebraska, USA), with a maximum spectral range of 0.75–5.15 eV, spectral point resolution of 0.001–0.022 eV, and operating on the dual rotating compensator principle (Chen *et al.*, 2004) was used for this investigation. The minimum data acquisition time for the full spectrum was 0.25 s, making this tool suitable for real-time monitoring in this application. Ellipsometric spectra (in Δ, ψ) were collected at room temperature (20 ± 1ºC) *via* RTSE monitoring during sample modification from reflection-mode measurements at an oblique angle of incidence of 70º. The spectral range was limited to 1.5–4.5 eV due to the absorption of light by water (H_2O). A representative surface was placed at the bottom of a fused silica vessel with windows at 70º to the sample surface such that the incident light from the ellipsometer passed through the windows at normal incidence (Figure 2). After introducing 150 mL of polymer solution at a concentration of 1 g/L of PAM to the vessel, the polymer was allowed to adsorb onto the surface for 2 h. A 2 h time period was selected to allow the PAM to be adsorbed uniformly onto the representative surface as the amount of PAM adsorbed on a silica surface reached equilibrium within ~1 h (Stemme *et al.*, 1999). Consequently, the adsorption density was the same at all points on the surface. The solution pH was then adjusted to the selected target value of 3, 6, or 11.5. The RTSE monitoring was started after the pH adjustment and continued for ~24 h. After the last RTSE measurement, the solution pH was measured using an Accumet XL 50 pH meter with relative accuracy of ± 0.002 pH (Fisher Scientific). In addition to monitoring real-time changes in the PAM layer thickness, the thickness of the surface was monitored under the same conditions without PAM. SiO_2 dissolution was insignificant for the conditions tested, and thus only the dissolution of Al_2O_3 was measured using RTSE.

Analysis of PAM layer-thickness evolution

The time-dependent thickness variations and complex dielectric function, ε, of the PAM layer were extracted using a least-squares regression analysis and an unweighted error function (Cong *et al.*, 1991) to fit the experimental RTSE data using structural models. These models are layered structures consisting of (1) a semi-infinite c-Si wafer with a 1.7-nm thick layer of native

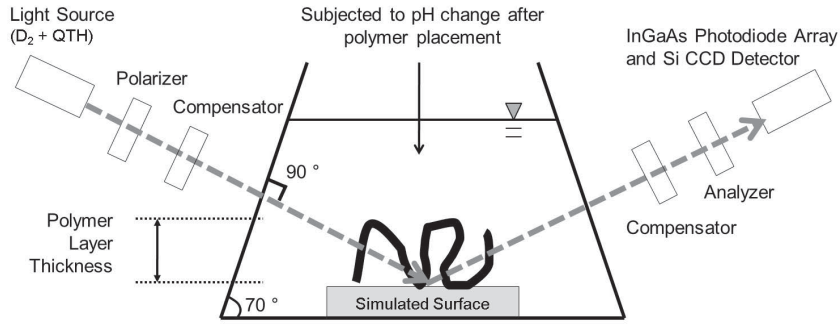

Figure 2. Schematic illustration of the spectroscopic ellipsometry apparatus for monitoring PAM swelling in real time.

SiO_2 and a PAM layer submerged in H_2O for monitoring the evolution of PAM on the amorphous SiO_2 surface and (2) a semi-infinite c-Si wafer with a 1.7-nm thick layer of native SiO_2 and a 39.7-nm thick layer of nanocrystalline Al_2O_3, along with a PAM layer submerged in H_2O for monitoring PAM on the nanocrystalline Al_2O_3 surface. For each sample, ε was obtained by fitting 8−10 individual SE measurements selected from the RTSE data to structural models where the PAM thickness can vary but a single common parameterization was used to describe ε. For PAM on amorphous SiO_2, this parameterization of ε consisted of a Sellmeier oscillator (Collins and Ferlauto, 2005) and a constant additive term to ε_1. Multiple SE measurements for PAM on the amorphous SiO_2 were selected throughout the time range of the experiment. The RTSE measurements of PAM on nanocrystalline Al_2O_3 surfaces did not yield the sensitivity to the dispersion of ε, so the average values over the 1.5−4.5 eV spectral range were obtained and the parameterization consisted of only the constant additive term to ε_1. Due to the etching of nanocrystalline Al_2O_3 by both HCl and NaOH, the thickness of Al_2O_3 was allowed to vary with time during the analysis of RTSE data, whereas the amorphous SiO_2 thickness remained fixed at its initial value. For PAM layers on Al_2O_3 where the pH was 6 and 3, multiple individual SE measurements selected from the first 2 h of RTSE data were analyzed using a single time-independent ε parameterization for the PAM layer, but allowing the PAM and Al_2O_3 layer thicknesses to vary for each set of ellipsometric spectra. For both pH = 3 and pH = 6, some Al_2O_3 was present throughout RTSE monitoring. For pH = 11.5, the Al_2O_3 was etched away rapidly during monitoring, so multiple individual ellipsometric spectra were collected near the end of monitoring to extract ε to avoid correlations between the PAM and Al_2O_3 layer thicknesses due to the rapid changes initially observed in the Al_2O_3 thickness. In this way, representative ε values for each film were obtained, which could then be used to determine the PAM thickness for all ellipsometric spectra collected in real time. The underlying native oxide thickness or initial nanocrystalline Al_2O_3 thickness was determined from a separate measurement of each coated c-Si wafer in air. Reference spectra in ε for native SiO_2, c-Si (Herzinger *et al.*, 1998), and H_2O (Synowicki *et al.*, 2004) were used. A Sellmeier oscillator and a constant additive term to ε_1 were used to parameterize ε for the nanocrystalline Al_2O_3 material prepared by ALD.

Swelling potential

The swelling potential of CPN may be a function of polymer conformation in the CPN. Therefore, the swelling potential of CPN synthesized using PAM can vary with pH and time. It was expected to increase with increasing pH and time following the extended conformation of PAM molecules. The difference between the nanocomposite and the microcomposite was the presence of interlayer adsorption of PAM molecules. The nanocomposite had PAM molecules adsorbed in the interlayer space of the montmorillonite particles. Because both interlayer and interparticle spacing can be modified by altering pH, the nanocomposite was expected to have a greater degree of change in swelling potential than that of the microcomposite.

The swelling potential was determined by measuring the water absorption capacity for dry powder CPN (Vazquez *et al.*, 1997; Bajpai and Giri, 2003; Mahdavinia *et al.*, 2004). The dry powder sample (1 g) was placed in a paper fiber filter bag of known weight and immersed in 250 mL of a pH-adjusted solution. The solution was prepared by mixing distilled water with 0.1 M HCl or NaOH solutions to target pH 3, 6, and 11.5. The sample was allowed to hydrate at room temperature. At pre-determined time intervals, the filter bag containing the swollen sample was allowed to drain by hanging until the sample no longer released free water droplets (~20 min). The filter bag was then weighed to determine the mass of the swollen gel. The swelling ratio was calculated by dividing the mass of the swollen sample by the mass of the dry sample. Note that swelling ratios for untreated clay minerals were obtained from the swell index (ASTM D5890, 2006) because the pore size of the filter bag was larger than the particles of

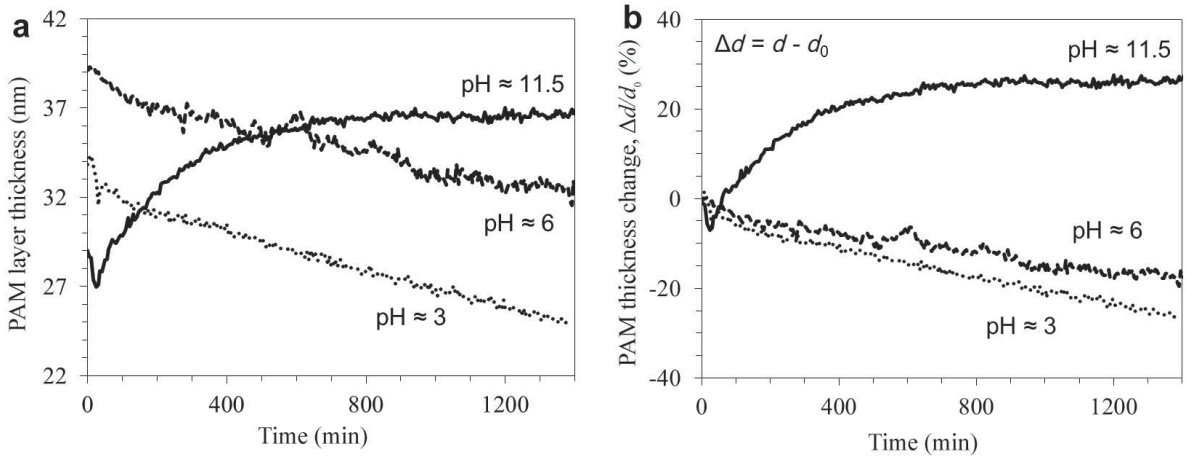

Figure 3. (a) Thickness of PAM adsorbed on the SiO_2 surface and (b) percentage change in the PAM thickness as a function of time in solution with pH = 3, 6, or 11.5.

the untreated clay mineral. The swelling ratio for untreated clay minerals was defined as the volumetric ratio of the soil sample before and after the sample was immersed in deionized water for 72 h.

RESULTS AND DISCUSSION

PAM conformation on the SiO_2 surface

The PAM layer thickness on SiO_2 for each solution pH over the span of 1 day was observed to be time dependent (Figure 3a). The initial thicknesses, d_0, of the PAM layers were different and ranged from 29 to 39 nm. The error on all thickness values was ±0.4 nm. The percentage difference in the thickness for each layer as a function of time (Figure 3b) was determined by $\Delta d = (d-d_0)/d_0$, where d is the PAM layer thickness at a given time and d_0 is the initial PAM layer thickness. No significant variation in ε_1 ($\varepsilon_2 = 0$) for PAM layers on SiO_2 was obtained regardless of the solution pH (Figure 4).

The PAM in the basic solution (pH = 11.5) was observed to swell by ~27% of the initial value after ~24 h, while the PAM in the acidic solutions (pH = 3 or 6) contracted by 26% or 17%, respectively. Closer investigation of the time-dependent PAM layer thickness showed that the thickness of PAM in the pH = 11.5 solution appeared to decrease initially in the first 15 min by 7%, and then increased subsequently throughout the remainder of the RTSE monitoring. The thickness of the PAM in the pH = 11.5 reached a maximum at ~600 min (10 h). The PAM layer thickness at pH = 6 decreased monotonically with time, although the PAM layer thickness in the more acidic solution (pH = 3) contracted more rapidly. The contraction rate for PAM in the pH = 6 solution appeared to stabilize somewhat after 900 min (15 h), indicating that a steady state may have been reached. PAM in the pH = 3 solution did not appear to stabilize over the measurement time.

The initial difference in the layer thickness ranging from 29 to 39 nm can be explained by a difference in ionic strength due to the addition of 0.1 M NaOH and HCl solution as a pH modifier. The concentration of Na^+ at pH = 11.5 was ~0.006 M, while that of Cl^- at pH = 3 was ~0.001 M. These concentrations were large enough to induce contracted coil conformation for PAM (Klenina and Lebedeva, 1983). Thus, PAM in the absence of added ions, *i.e.* at pH = 6, had the maximum initial layer thickness. Assuming that no additional PAM attached to the surface during this time, for pH = 11.5 solution the PAM was expected to have initially contracted on the SiO_2 surface, but later uncoiled resulting in the increased layer thickness. After 15 min, expansion of the PAM molecules offset the initial decrease. The PAM in pH = 3 and 6 solutions began as constricted and coiled near the SiO_2 surface and continued to contract. For pH = 6, however, changes in the layer thickness stabilized after 15 h, while the PAM thickness for pH = 3 continued to

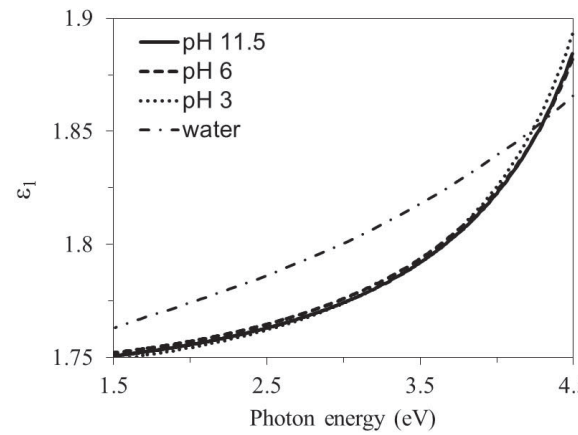

Figure 4. Real part of the complex dielectric function spectra ($\varepsilon = e_1 + i\varepsilon_2$) for PAM on SiO_2 in solution with pH = 3, 6, or 11.5. Also shown is ε_1 for water.

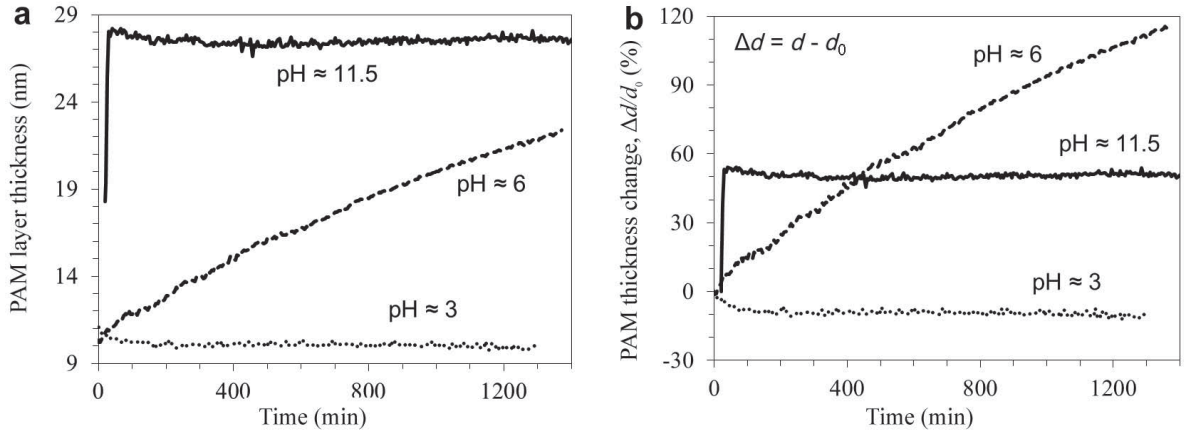

Figure 5. (a) Thickness of PAM adsorbed on the Al_2O_3 surface and (b) percentage change in the PAM thickness as a function of time in solution with pH = 3, 6, or 11.5.

decrease. Although the layer thickness was expected to remain nearly constant at pH = 3 and 6, this unexpected time-dependent phenomenon at these pH values can be explained through the concept of surface coverage. The adsorbed polymer layer thickness has been reported to decrease with increasing surface coverage, and a large-molecular-weight polymer adsorbed on a surface slowly covered the surface (Leermakers *et al.*, 1996; Filippova, 1998; Samoshina *et al.*, 2005). At all pH values tested, the same surface-covering behavior occurred to different degrees due to pH-dependent charges on the PAM molecules. Because surface coverage increases with decreasing intermolecular repulsion (Leermakers *et al.*, 1996), the surface coverage at pH = 3 was at a maximum leading to the minimum polymer layer thickness. In theory, the surface coverage at pH = 6 should be nearly the same as at pH = 3. However, in reality, PAM molecules usually have slightly negative charges at neutral pH caused by a finite degree of hydrolysis of amide groups into acrylic acid (Kurenkov, 1997) such that the PAM molecules have a slightly expanded coiled conformation.

PAM conformation on the Al_2O_3 surface

The PAM layer thickness on the Al_2O_3 surface was monitored as a function of time and pH (Figure 5a). The percentage differences at various times and pH values tested were also calculated (Figure 5b). The Al_2O_3 thickness (Figure 6a) and the percentage difference in the Al_2O_3 thickness (Figure 6b) for each solution pH over ~24 h were also determined. As the dispersion of ε was not obtainable for PAM layers on Al_2O_3, values of ε_1 were 2.05±0.15, 1.69±0.01, and 1.76±0.01 for pH = 3, 6, and 11.5, respectively.

A monotonic increase in the PAM layer thickness as well as a decrease in Al_2O_3 thickness with time were observed at pH = 6. The effective PAM layer thickness increased from 10.3 nm to 22.3 nm, while the Al_2O_3 thickness decreased from 39.6 to 28.8 nm. This behavior was an effective increase in PAM layer thickness of

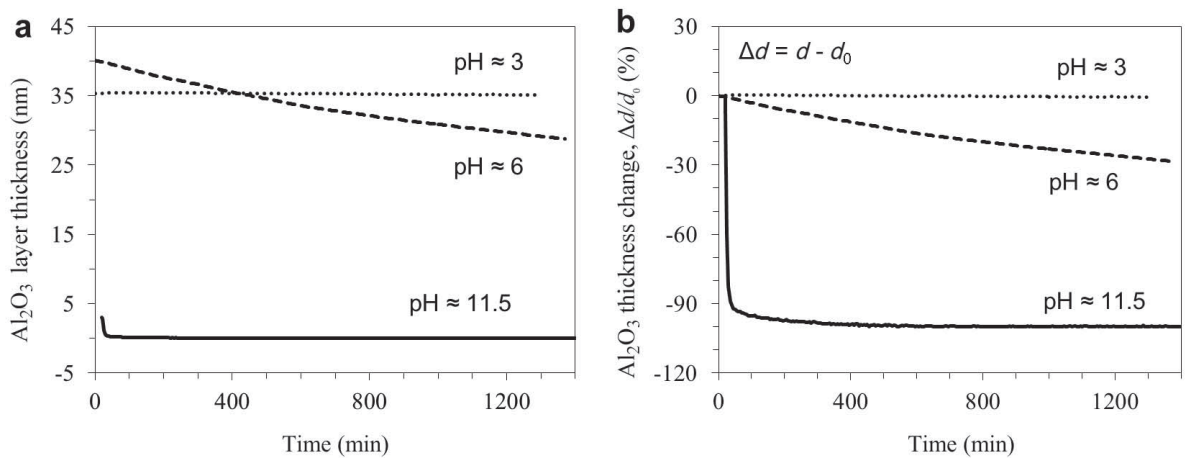

Figure 6. (a) Thickness of the Al_2O_3 layer and (b) percentage change in the Al_2O_3 thickness as a function of time in solution with pH = 3, 6, or 11.5.

117% of the initial value and a 28% decrease in Al_2O_3 thickness. For the pH = 3 solution, the thickness of the alumina surface initially decreased from 39.7 to 35.3 nm. However, after this initial reduction, the thickness of the Al_2O_3 surface decreased only slightly (<1.0% change) throughout the remainder of RTSE monitoring. The PAM thickness also decreased slightly throughout the experiment from 11 to 9.8 nm. The PAM layer in the pH = 3 solution exhibited a significantly smaller variation (~10% change) than that of the pH = 6 case. For the pH = 11.5 solution, the Al_2O_3 surface was etched rapidly to a thickness of 3 nm during the first 20 min and decreased continuously until it was completely consumed. The PAM layer thickness increased during the first 20−30 min from 18.2 to 28 nm (52% increase) then stabilized for the remainder of the experiment. Unlike PAM on the SiO_2 surface at pH = 11.5, measurements taken prior to 20 min into the experiment could not be analyzed due to a lack of sufficient data points and the rapid changes occurring in the Al_2O_3 layer thickness. Relative changes were determined by comparing the PAM and Al_2O_3 thicknesses with those obtained after 20 min of immersion.

In contrast to the behavior observed on the SiO_2 surface, the thickness of the PAM layer on Al_2O_3 increased with time at pH = 6. In addition, ε_1 was less for PAM in solution at pH = 6 on Al_2O_3 than on SiO_2. A smaller ε_1 value means that light is refracted less by that material. A smaller ε_1 value, coinciding with a decrease in the index of refraction $n = e_1^{1/2}$ when $\varepsilon_2 = 0$, indicates that a less densely packed layer was formed on the Al_2O_3 substrate in this case. The surface coverage effect can be minimized for the case of PAM adsorption onto the Al_2O_3 surface. Because alumina is a hydrophilic oxide, PAM molecules can cover the whole surface in a relatively small amount of time. In agreement with this observation, alumina surface coverage for PAM molecules was fully achieved after a 2 h adsorption period prior to the pH adjustment. Due to the greater surface coverage than on the SiO_2 surface, train conformation of the polymer molecules became dominant on the Al_2O_3 surface after the adsorption period. The dominant conformation of the polymer molecules on the SiO_2 surface was loop conformation. The density of polymer molecules with loop conformation is less than that of the train-conformation dominant system (Fleer, 1993). Thus, the monotonic increase in the PAM layer thickness can be explained by hydrolysis behavior of PAM at near-neutral pH. As the amide group of PAM molecules hydrolyzes into acrylic acid, PAM molecules become slightly negatively charged leading to intermolecular expansion (Kurenkov, 1997). Because neutral hydrolysis is not an instant reaction, the intermolecular expansion was time dependent, resulting in an increase in the PAM layer thickness over time.

Unlike silica, the solubility of which is nearly independent of pH and insignificant for a time period of 1 day, alumina is a hydrophilic oxide with pH-dependent solubility (Snoeyink and Jenkins, 1980; Wehrli *et al.*, 1990; Stumm, 1992). Hence, alumina dissolution must be considered for the pH conditions tested. In general, alumina dissolution should be minimal at pH $\approx$ 6 and increase with increasing or decreasing pH. The dissolution rates of the alumina determined by immersing Al_2O_3-coated wafers in solution without the PAM used in the present study were −0.00166 nm/min at pH = 3 and −0.1654 nm/min at pH = 11.5, while the surface had the opposite charge; negatively charged at pH = 11.5 *vs.* positively charged at pH = 3. A significant difference in the Al_2O_3 layer thickness was observed, however, between pH = 3 and pH = 11.5 solutions with PAM. Based on the observation of PAM layer thickness, the difference in Al_2O_3 thickness may be attributed to PAM adsorption, which alters dissolution of the Al_2O_3 surface. As in the case of the SiO_2 surface, adsorbed PAM molecules tend to have contracted coiled conformation at pH = 3, leading to a decrease in the PAM layer thickness. Therefore, the PAM molecules adsorbed were densely linked, forming a film-like coating on the Al_2O_3 surface. On the other hand, extended PAM molecules at pH=11.5 were weakly linked or freely extended from the surface, allowing water molecules with OH^- to contact the surface and leading to dissolution of the entire Al_2O_3 layer. The greater value of ε_1 for the PAM layer at pH = 3 also indicated that the molecules on the surface may have been more densely packed and formed a somewhat etch-resistant coating on the Al_2O_3 surface (Jaffe, 1956).

The conformational change of adsorbed PAM molecules exposed to strong acid or strong base (Figure 5a) took place relatively quickly compared to the SiO_2 surface (Figure 3a). This behavior may be due to dissolved Al ions, which played a significant role in the conformational behavior of PAM. Based on the solution pH measurement at the end of RTSE monitoring, the dissolved Al ions may have interacted with the polymer molecules. For the SiO_2 surface, the solution pH decreased from 11.52 to 10.57 (a difference of 0.95), while the solution pH for the Al_2O_3 surface decreased from 11.51 to 10.12 (a difference of 1.39). Because the hydrolysis reaction of PAM requires OH^-, the solution pH tended to decrease for pH = 11.5 regardless of surface type. The magnitude of the decrease observed for the Al_2O_3 case was, however, greater than that of the SiO_2 case. Dissolved Al ions interact with hydrolyzed groups of a PAM molecule forming $Al(R\text{-}COO)_3$ complexes and releasing H^+ ions (Ringenbach *et al.*, 1995). Thus, the solution pH decreased further when using the Al_2O_3 surface due to the formation of these complexes. Based on the observation that the PAM conformation changed more rapidly in the presence of dissolved Al ions, the dissolved Al ions probably promoted the PAM hydrolysis reaction resulting in more rapid conformational changes.

The PAM layer thickness measurements for pH = 6, using SiO_2 and Al_2O_3 surfaces were also consistent with Al ion interactions with PAM. The PAM layer thickness on the SiO_2 surface was ~33% greater at pH = 6 than at pH = 3, while the PAM layer thickness on the Al_2O_3 surface was ~126% greater at pH = 6 than at pH = 3. The dissolved aluminum ions probably promoted PAM hydrolysis reactions at near-neutral pH as well as at high pH. Quantitative changes in the kinetics of PAM conformation evolution cannot be ascertained due to many factors simultaneously affecting the conformational behavior, such as counterion binding, controlled complexation, and modified hydrophilicity due to the continuous oxide dissolution, as well as charge screening effects which are similar to those developed by the addition of HCl or NaOH solutions (Ikegami and Imai, 1962; Spencer, 1962; Klenina and Lebedeva, 1983; Wehrli *et al.*, 1990; Ringenbach *et al.*, 1993).

Swelling potential

The swelling ratio determined by measuring water adsorption capacity tends to increase with time at all tested pH values until reaching equilibrium (Figure 7), but the magnitude differed significantly between the micro- and nanocomposites. After 72 h, the nanocomposite and microcomposite at pH = 11.5 had swelling ratios of 12.9 and 1.45, respectively, while those at pH = 3 had swelling ratios of ~3.8 and 1.1, respectively. The measured degree of hydrolysis for the polymer at pH = 11.5 was 0.81, which was in good agreement with reported experimental values of maximum degree of hydrolysis (Kurenkov, 1997; Huang *et al.*, 2001). As expected, the PAM hydrolysis rate was greater under basic conditions (Kheradmand *et al.*, 1988; Kurenkov, 1997). Swelling ratios for both CPN types increased more rapidly at pH = 11.5 than at a lower value. The difference in swelling ratio between samples at pH = 3 and 6 was expected to be insignificant because little ionization occurs at pH < 8.5, *i.e* ~2 units lower than the pK_a value. However, PAM hydrolysis at neutral pH, as well as the addition of 0.1 M HCl solution to adjust the solution pH, may have contributed to the observed difference seen in both CPN.

Equilibrium swelling ratios for untreated clay minerals were reached after 24 h. The swelling ratio for untreated kaolinite was 1 at all tested pH conditions, while that for untreated montmorillonite was 11.7 at pH = 3, 12 at pH = 6, and 11.5 at pH = 11.5. Montmorillonite swelling decreased with increasing ionic strength (Abdullah *et al.*, 1999; Karnland *et al.*, 2007; Herbert *et al.*, 2008). Thus, the slightly pH-dependent swelling ratio was probably due to increased ionic concentration by adding 0.1 M HCl or NaOH solution as a pH modifier. Expansion of polymer conformation was also limited by high ionic strength at high and low pH (Aulich *et al.*, 2010; Bittrich *et al.*, 2010). Thus, the same effect probably occurred in the swelling ratio measurement for both CPN. However, when comparing the extent of PAM conformation-induced swelling, the effect of increased ionic strength was insignificant after equilibrium was reached.

These swelling results are in reasonable agreement with the studies of PAM on the representative surfaces by RTSE. PAM uncoils and expands in basic solutions and coils and contracts to different degrees in acidic solutions. In spite of previously reported results that polymer treatment limits swelling behavior (Inyang *et al.*, 2007), the swelling ratio results for the CPN implied that conformational changes of PAM adsorbed on the CPN led to interlayer and/or interparticle spacing changes. PAM-induced interlayer and interparticle spacing changes were expected for the nanocomposite, while only interparticle spacing change was likely for the microcomposite. However, the magnitude of interlayer swelling and interparticle swelling due to PAM conformation changes cannot be separated because the

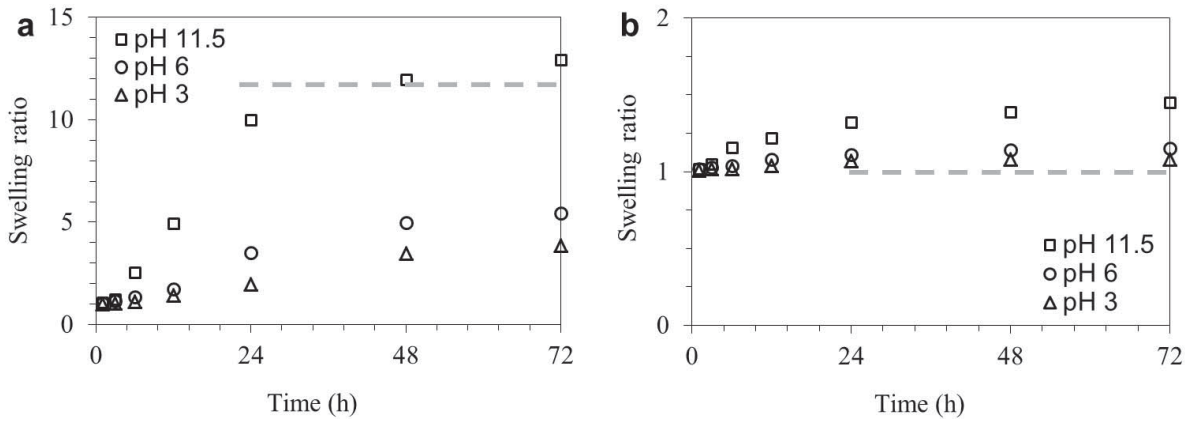

Figure 7. Swelling ratio of clay polymer nanocomposite (CPN) as a function of pH and time: (a) montmorillonite-PAM nanocomposite and (b) kaolinite-PAM microcomposite. The dashed line denotes the swelling ratio for the untreated clay mineral (pH = 6 in the case of the montmorillonite-PAM nanocomposite).

swelling behavior depends on many factors such as mineral composition, grain size, aggregate size, cation exchange capacity, and chemical composition and concentration of the bulk fluid (Shackelford *et al.*, 2000; Ashmawy *et al.*, 2002). Nevertheless, the results indicated that both interlayer and interparticle spacings can be modified by a pH-responsive polymer. Another important finding from the results was that the swelling property of CPN synthesized with a pH-responsive polymer can be controlled by altering the pH condition such that the swelling was either less than or greater than that of the untreated material (Figure 7a).

CONCLUSIONS

In the present study RTSE and swelling potential measurements were used to: (1) investigate time-dependent conformational behavior of a pH-responsive polymer on two representative clay mineral surfaces; and (2) link the micro-scale responses to a meso-scale property, swelling, of CPN.

Time-dependent changes in layer thickness of adsorbed PAM with pH indicated that, for basic solutions (pH = 11.5), PAM uncoiled and expanded with time on both of the representative surfaces – amorphous SiO_2 and nanocrystalline Al_2O_3. The PAM layer thickness for the highly acidic solution (pH = 3) decreased with time, indicating coiling on the representative surfaces. However, PAM conformation reached the equilibrium state very rapidly on the Al_2O_3 surface due to the interactions of dissolved Al ions with the polymer molecules. The behavior of the intermediate, slightly acidic solution (pH = 6) showed conformational constriction on the SiO_2 surface and expansion on the Al_2O_3 surface.

The RTSE results on the micro-scale PAM conformations were in reasonable agreement with the measured meso-scale swelling potential of CPN – both the nanocomposite and the microcomposite. This corresponded to the conformational behavior of PAM varying with solution pH. The swelling potential of CPN was controlled by adjusting the pH condition such that the swelling was either less than or greater than that of the untreated clay minerals.

Because the PAM conformation on a real clay-mineral surface may be different from that on representative surfaces, a quantitative linkage between the micro-scale PAM conformation and the meso-scale swelling behavior of CPN was not made. Nevertheless, insights into how conformation of adsorbed PAM on silica and alumina surfaces varies with pH and time were achieved.

ACKNOWLEDGMENTS

This study was based upon work supported by the National Science Foundation under Grant No. 1041995. Funding was also provided by the Materials Research Institute at the Pennsylvania State University. Nanocrystalline Al_2O_3 layers were kindly provided by the research group of Prof. Thomas N. Jackson in the Department of Electrical Engineering at Pennsylvania State University.

REFERENCES

Abdullah, W.S., Alshibli, K.A., and Al-Zou'bi, M.S. (1999) Influence of pore water chemistry on the swelling behavior of compacted clays. *Applied Clay Science*, **15**, 447–462.

Al-Anazi, H.A. and Sharma, M.M. (2002) Use of a pH sensitive polymer for conformance control. *International Symposium and Exhibition on Formation Damage Control*, Lafayette, Louisiana.

Alexandre, M. and Dubois, P. (2000) Polymer-layered silicate nanocomposites: Preparation, properties and uses of a new class of materials. *Materials Science and Engineering: R: Reports*, **28**, 1–63.

Ashmawy, A.K., El-Hajji, D., Sotelo, N., and Muhammad, N. (2002) Hydraulic performance of untreated and polymer-treated bentonite in inorganic landfill leachates. *Clays and Clay Minerals*, **50**, 546–552.

Askadskii, A.A. (1990) Influence of crosslinking density on the properties of polymer networks. *Polymer Science U.S.S.R.*, **32**, 2061–2069.

ASTM (2006) *D5890: Standard test method for swell index of clay mineral component of geosynthetic clay liners*. American Society for Testing and Materials (ASTM).

Aulich, D., Hoy, O., Luzinov, I., Brucher, M., Hergenroder, R., Bittrich, E., Eichhorn, K.-J., Uhlmann, P., Stamm, M., Esser, N., and Hinrichs, K. (2010) In situ studies on the switching behavior of ultrathin poly(acrylic acid) polyelectrolyte brushes in different aqueous environments. *Langmuir*, **26**, 12926–12932.

Bajpai, A.K. and Giri, A. (2003) Water sorption behaviour of highly swelling (carboxy methylcellulose-g-polyacrylamide) hydrogels and release of potassium nitrate as agrochemical. *Carbohydrate Polymers*, **53**, 271–279.

Barvenik, F.W. (1994) Polyacrylamide characteristics related to soil applications. *Soil Science*, **158**, 235–243.

Besra, L., Sengupta, D.K., Roy, S.K., and Ay, P. (2004) Influence of polymer adsorption and conformation on flocculation and dewatering of kaolin suspension. *Separation and Purification Technology*, **37**, 231–246.

Bittrich, E., Kuntzsch, M., Eichhorn, K.-J., and Uhlmann, P. (2010) Complex pH- and temperature-sensitive swelling behavior of mixed polymer brushes. *Journal of Polymer Science Part B: Polymer Physics*, **48**, 1606–1615.

Borchardt, G. (1989) Smectites. Pp. 675–727 in: *Minerals in Soil Environments* (J.B. Dixon, S.B. Weed, and R.C. Dinauer, editors). Soil Science Society of America, Madison, Wisconsin, USA.

Caskey, J.A. and Primus, R.J. (1986) The effect of anionic polyacrylamide molecular conformation and configuration on flocculation effectiveness. *Environmental Progress*, **5**, 98–103.

Castel, D., Ricard, A., and Audebert, R. (1990) Swelling of anionic and cationic starch-based superabsorbents in water and saline solution. *Journal of Applied Polymer Science*, **39**, 11–29.

Chen, C., An, I., Ferreira, G.M., Podraza, N.J., Zapien, J.A., and Collins, R.W. (2004) Multichannel Mueller matrix ellipsometer based on the dual rotating compensator principle. *Thin Solid Films*, **455-456**, 14–23.

Cohen Stuart, M.A., Cosgrove, T., and Vincent, B. (1986) Experimental aspects of polymer adsorption at solid/solution interfaces. *Advances in Colloid and Interface Science*, **24**, 143–239.

Collins, R.W. and Ferlauto, A.S. (2005) Optical properties of

materials. Pp. 125–129 in: *Handbook of Ellipsometry* (H.G. Tompkins and E.A. Irene, editors). William Andrew Publisers, Springer, Norwich, New York, USA.

Cong, Y., An, I., Vedam, K., and Collins, R.W. (1991) Optical characterization of a four-medium thin film structure by real time spectroscopic ellipsometry: amorphous carbon on tantalum. *Applied Optics*, **30**, 2692–2703.

Fan, X. and Advincula, R.C. (2002) Nanostructured ultrathin films of silicate clay and polyelectrolytes: deposition parameters and mechanical properties by nanoindentation. *Materials Research Society Symposium Proceedings*, Boston, Massachusetts, USA, pp. 335–340.

Fan, X., Park, M.-k., Xia, C., and Advincula, R. (2002) Surface structural characterization and mechanical testing by nanoindentation measurements of hybrid polymer/clay nanostructured multilayer films. *Journal of Materials Research*, **17**, 1622–1633.

Filippova, N.L. (1998) Adsorption and desorption kinetics of polyelectrolytes on planar surfaces. *Langmuir*, **14**, 1162–1176.

Fleer, G.J. (1993) *Polymers at Interfaces*, 1st edition. Chapman & Hall, London, New York.

Flory, P.J. (1953) *Principles of Polymer Chemistry*. Cornell University Press, Ithaca, New York.

Furusawa, K., Shou, Z., and Nagahashi, N. (1992) Polymer adsorption on fine particles; the effects of particle size and its stability. *Colloid and Polymer Science*, **270**, 212–218.

Giannelis, E.P., Krishnamoorti, R., and Manias, E. (1999) Polymer-silicate nanocomposites: Model systems for confined polymers and polymer brushes. *Advances in Polymer Science*, **138**, 107–147.

Gupta, P., Vermani, K., and Garg, S. (2002) Hydrogels: from controlled release to pH-responsive drug delivery. *Drug Discovery Today*, **7**, 569–579.

Herbert, H.-J., Kasbohm, J., Sprenger, H., Fernandez, A.M., and Reichelt, C. (2008) Swelling pressures of MX-80 bentonite in solutions of different ionic strength. *Physics and Chemistry of the Earth*, **33**, S327–S342.

Herzinger, C.M., Johs, B., McGahan, W.A., Woollam, J.A., and Paulson, W. (1998) Ellipsometric determination of optical constants for silicon and thermally grown silicon dioxide via a multi-sample, multi-wavelength, multi-angle investigation. *Journal of Applied Physics*, **83**, 3323–3336.

Huang, S.-Y., Lipp, D.W., and Farinato, R.S. (2001) Acrylamide polymers. Pp. 304–342 in: *Kirk-Othmer Encyclopedia of Chemical Technology* (A. Seidel, editors). John Wiley & Sons, New Jersey, USA.

Ikegami, A. and Imai, N. (1962) Precipitation of polyelectrolytes by salts. *Journal of Polymer Science*, **56**, 133–152.

Inyang, H.I., Bae, S., Mbamalu, G., and Park, S.-W. (2007) Aqueous polymer effects on volumetric swelling of Na-montmorillonite. *Journal of Materials in Civil Engineering*, **19**, 84–90.

Irene, E.A. (1993) Applications of spectroscopic ellipsometry to microelectronics. *Thin Solid Films*, **233**, 96–111.

Jaffe, H.W. (1956) Application of the rule of gladstone and dale to minerals. *American Mineralogist*, **41**, 757.

Karnland, O., Olsson, S., Nilsson, U., and Sellin, P. (2007) Experimentally determined swelling pressures and geochemical interactions of compacted Wyoming bentonite with highly alkaline solutions. *Physics and Chemistry of the Earth*, **32**, 275–286.

Kheradmand, H., Francois, J., and Plazanet, V. (1988) Hydrolysis of polyacrylamide and acrylic acid-acrylamide copolymers at neutral pH and high temperature. *Polymer*, **29**, 860–870.

Kim, S. (2011) An engineered clay soil system using functional polymers. Ph.D. dissertation, Pennsylvania State University, University Park, Pennsylvania, USA.

Kim, S. and Palomino, A.M. (2009) Polyacrylamide-treated kaolin: A fabric study. *Applied Clay Science*, **45**, 270–279.

Kim, S. and Palomino, A. M. (2011) Factors influencing the synthesis of tunable clay-polymer nanocomposites using bentonite and polyacrylamide. *Applied Clay Science*, **51**, 491–498.

Kim, S., Palomino, A.M., and Colina, C.M. (2012) Responsive polymer conformation and resulting permeability of clay-polymer nanocomposites. *Molecular Simulation*, **38**, 723–734

Klenina, O.V. and Lebedeva, L.G. (1983) Viscometric properties of dilute solutions of hydrolyzed polyacrylamide. *Polymer Science U.S.S.R.*, **25**, 2380–2389.

Kurenkov, V.F. (1997) Acrylamide polymers. Pp. 61–72 in: *Handbook of Engineering Polymeric Materials* (N.P. Cheremisinoff, editors). Marcel Dekker, New York.

Lee, J.J. and Fuller, G.G. (1984) Ellipsometry studies of adsorbed polymer chains subjected to flow. *Macromolecules*, **17**, 375–380.

Lee, J.W., Kim, S.Y., Kim, S.S., Lee, Y.M., Lee, K.H., and Kim, S.J. (1999) Synthesis and characteristics of interpenetrating polymer network hydrogel composed of chitosan and poly(acrylic acid). *Journal of Applied Polymer Science*, **73**, 113–120.

Lee, W.-F. and Lin, G.-H. (2001) Superabsorbent polymeric materials VIII: Swelling behavior of crosslinked poly[sodium acrylate-co-trimethyl methacryloyloxyethyl ammonium iodide] in aqueous salt solutions. *Journal of Applied Polymer Science*, **79**, 1665–1674.

Leermakers, F.A.M., Atkinson, P.J., Dickinson, E., and Horne, D.S. (1996) Self-consistent-field modeling of adsorbed [beta]-casein: effects of pH and ionic strength on surface coverage and density profile. *Journal of Colloid and Interface Science*, **178**, 681–693.

Mahdavinia, G.R., Pourjavadi, A., Hosseinzadeh, H., and Zohuriaan, M.J. (2004) Modified chitosan 4. Superabsorbent hydrogels from poly(acrylic acid-co-acrylamide) grafted chitosan with salt- and pH-responsiveness properties. *European Polymer Journal*, **40**, 1399–1407.

Michaels, A.S. (1954) Aggregation of suspensions by polyelectrolytes. *Industrial & Engineering Chemistry*, **46**, 1485–1490.

Myagchenkov, V.A. and Proskurina, V.E. (2004) Flocculation activity (with respect to ocher) of anionic copolymers of acrylamide in the mode of restricted sedimentation as influenced by their chemical heterogeneity. *Russian Journal of Applied Chemistry*, **77**, 463–466.

Pefferkorn, E. (1999) Polyacrylamide at solid/liquid interfaces. *Journal of Colloid and Interface Science*, **216**, 197–220.

Ray, S.S. and Okamoto, M. (2003) Polymer/layered silicate nanocomposites: a review from preparation to processing. *Progress in Polymer Science*, **28**, 1539–1641.

Ringenbach, E., Chauveteau, G., and Pefferkorn, E. (1993) Adsorption of polyelectrolytes on soluble oxides induced by polyion complexation with dissolution species. *Journal of Colloid and Interface Science*, **161**, 223–231.

Ringenbach, E., Chauveteau, G., and Pefferkorn, E. (1995) Effect of soluble aluminum ions on polyelectrolyte-alumina interaction. Kinetics of polymer adsorption and colloid stabilization. *Colloids and Surfaces A: Physicochemical and Engineering Aspects*, **99**, 161–173.

Ruiz-Hitzky, E. and van Meerbeek, A. (2006) Clay mineral- and organoclay-polymer nanocomposite. Pp. 141–245 in: *Handbook of Clay Science* (F. Bergaya, B.K.G. Theng, and G. Lagaly, editors). Elsevier, Amsterdam.

Russev, S.C., Arguirov, T.V., and Gurkov, T.D. (2000) [beta]-Casein adsorption kinetics on air-water and oil-water interfaces studied by ellipsometry. *Colloids and Surfaces B: Biointerfaces*, **19**, 89–100.

Samoshina, Y., Nylander, T., Shubin, V., Bauer, R., and Eskilsson, K. (2005) Equilibrium aspects of polycation adsorption on silica surface: How the adsorbed layer responds to changes in bulk solution. *Langmuir*, **21**, 5872–5881.

Schmidt, D.J., Cebeci, F.C., Kalcioglu, Z.I., Wyman, S.G., Ortiz, C., Van Vliet, K.J., and Hammond, P.T. (2009) Electrochemically controlled swelling and mechanical properties of a polymer nanocomposite. *ACS Nano*, **3**, 2207–2216.

Schwarz, S., Eichhorn, K.J., Wischerhoff, E., and Laschewsky, A. (1999) Polyelectrolyte adsorption onto planar surfaces: a study by streaming potential and ellipsometry measurements. *Colloids and Surfaces A: Physicochemical and Engineering Aspects*, **159**, 491–501.

Shackelford, C.D., Benson, C.H., Katsumi, T., Edil, T.B., and Lin, L. (2000) Evaluating the hydraulic conductivity of GCLs permeated with non-standard liquids. *Geotextiles and Geomembranes*, **18**, 133–161.

Shubin, V. and Linse, P. (1995) Effect of electrolytes on adsorption of cationic polyacrylamide on silica: Ellipsometric study and theoretical modeling. *The Journal of Physical Chemistry*, **99**, 1285–1291.

Snoeyink, V.L. and Jenkins, D. (1980) *Water Chemistry*. John Wiley & Sons, New York, Singapore.

Spencer, H.G. (1962) A note on dissociation constants of polycarboxylic acids. *Journal of Polymer Science*, **56**, S25–S28.

Stemme, S., Odberg, L., and Malmsten, M. (1999) Effect of colloidal silica and electrolyte on the structure of an adsorbed cationic polyelectrolyte layer. *Colloids and Surfaces A: Physicochemical and Engineering Aspects*, **155**, 145–154.

Strawhecker, K.E. and Manias, E. (2006) Nanocomposites based on water soluble polymers and unmodified smectite clays. Pp. 206–233 in: Polymer nanocomposites (Y.W. Mai and Z.-Z. Yu, editors). CRC Press, Boca Raton, Florida, USA.

Stumm, W. (1992) *Chemistry of the Solid-Water Interface: Processes at the Mineral-Water and Particle-Water Interface in Natural Systems*. Wiley, New York.

Synowicki, R.A., Pribil, G.K., Cooney, G., Herzinger, C.M., Green, S.E., French, R.H., Yang, M.K., Burnett, J.H., and Kaplan, S. (2004) Fluid refractive index measurements using rough surface and prism minimum deviation techniques. *Journal of Vacuum Science & Technology B*, **22**, 3450–3453.

van Olphen, H. (1977) *An Introduction to Clay Colloid Chemistry: For Clay Technologists, Geologists, and Soil Scientists.* Wiley, New York.

Vazquez, B., Roman, J.S., Peniche, C., and Cohen, M.E. (1997) Polymeric hydrophilic hydrogels with flexible hydrophobic chains. Control of the hydration and interactions with water molecules. *Macromolecules*, **30**, 8440–8446.

Wang, J., Wang, D.Y., Li, F., Tang, X.G., Chan, H.L.W., Mo, D., and Choy, C.L. (2004) Simple transmission ellipsometry method for measuring the electric-field-induced birefringence in PLZT thin films. *Journal of Materials Science*, **39**, 1805–1807.

Wehrli, B., Wieland, E., and Furrer, G. (1990) Chemical mechanisms in the dissolution kinetics of minerals; the aspect of active sites. *Aquatic Sciences*, **52**, 3–31.

Wu, J., Lin, J., Li, G., and Wei, C. (2001) Influence of the COOH and COONa groups and crosslink density of poly(acrylic acid)/montmorillonite superabsorbent composite on water absorbency. *Polymer International*, **50**, 1050–1053.

(*Received 6 February 2012; revised 26 June 2012; Ms. 652; A.E. F. Bergaya*)